Mathematical Modeling for the Window to the Brain: application of the Hybrid Digital Twins to enhance precision

Marcos Llamazares López[♭],[1] Juan-Carlos Cortés[♭], Macarena Trujillo Guillén[♮] and Rafael-Jacinto Villanueva[♭]

(♭) I.U. de Matemática Multidisciplinar, Universitat Politècnica de València
Camí de Vera s/n, València, Spain.

(♮) BioMIT, Department of Applied Mathematics, Universitat Politècnica de València
Camí de Vera s/n, València, Spain.

1 Introduction

The Window to the Brain (WttB) [1] is a prototype of a cranial implant whose objective is to provide optical access to the brain for minimally invasive laser treatments, like Laser Interstitial Thermal Therapies (LITT). The LITT utilize laser irradiation to treat malignancies like brain tissue tumors [2]. Mathematical modeling of this implant [3] is crucial for understanding its properties and improving its effectiveness.

In the modeling of the WttB there are two important issues: the management of uncertain parameters and the validation of the theoretical model comparing with experimental data which also presents some uncertain data. Taking into account that the range of temperature increase in brain tissue is crucial, the accuracy of the mathematical model is essential. The traditional method of enhancing modeling accuracy involves increasing model complexity, which often leads to problems such as over-fitting and difficulties in results interpretation.

This study explores an alternative approach to improving model accuracy without adding complexity to the equations. Hybrid Digital Twins (HDT) [4] integrate the classical model results with the novelty of Artificial Intelligence tools. Specifically, the model error is defined as the difference between the model output and experimental data, and this error is subsequently adjusted using Artificial Intelligence techniques. These results can then be utilized to make predictions.

2 Methods

2.1 Experimental Data

The experimental data utilized in this study is obtained from [3] and comprises temperature profiles for the surface of the WttB, acquired via thermal cameras during three separate experiments.

[1] marllalo@upvnet.upv.es

In Experiment 1, a single laser pulse was conducted, involving an exposure time of 40 seconds followed by a cooling period of 15 seconds. Experiment 2 employed a pulsed protocol, comprising five repetitive cycles with a 10-second exposure time and a 5-second cooling time. Experiment 3 replicated Experiment 2's setup, except for an extension of the cooling time to 10 seconds.

This data is divided into Training, Validation, and Test datasets. The Training dataset includes the data from Experiment 1 and the first cycle of Experiment 2. The Validation dataset comprises the data from the last 4 cycles of Experiment 2. Lastly, the Test dataset includes the data from Experiment 3.

2.2 Mathematical Model

The geometry of the WttB is a 2D-axisymmetric disk as depicted in Figure 1.

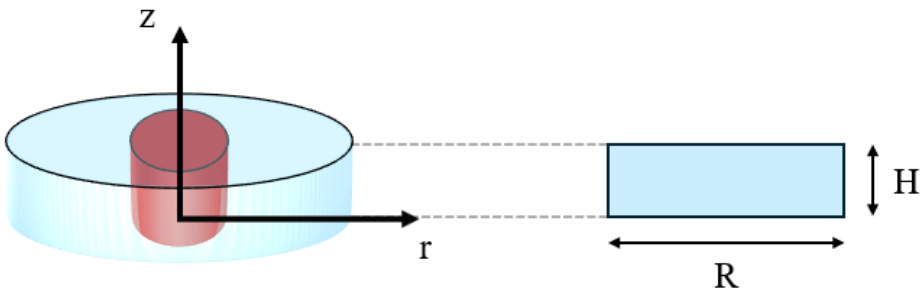

Figure 1: Schematic geometry of the WttB where the blue disk represents the biomedical implant and the red cylinder represents the laser source for LITT. R is the radius of the disk and H is the height.

The mathematical model [3] consists of a system of coupled differential equations designed to simulate a thermal-optical problem. The temperature dynamics was modeled using the Bioheat equation.

$$\rho c \frac{\partial T}{\partial t} = \nabla(k \nabla T) + Q \tag{1}$$

T being the material temperature, t time, ρ density, c specific heat, k thermal conductivity, and Q the heat generated by laser irradiation.

The Beer-Lambert equation (2) was employed to model the optical phenomenon, describing the absorption of laser irradiation by the sample.

$$\frac{\partial I}{\partial z} = -\alpha I, \tag{2}$$

where I represents the laser intensity, α the absorption coefficient of the material, and z the direction of laser propagation. The thermal and optical problems described by equations (1) and (2) are coupled by the equation

$$Q = \frac{\partial I}{\partial z}\,. \tag{3}$$

The parameters in the equations are calibrated utilizing a Particle Swarm Optimization (PSO) algorithm [5], utilizing the data in the Training dataset.

2.3 Hybrid Digital Twins (HDT)

The HDT methodology [4] utilizes both experimental data and the output from the classical model as inputs. The Error is computed as the difference between these inputs. An Artificial Intelligence tool, which in this study is a Grammatical Evolution [6] with Lexicase Selection [7], is employed to generate a fitting for the Error using the Training dataset. This fitting is then validated using the Validation dataset before being applied to make predictions within the Test dataset.

Finally, the output of the HDT is

$$H(X, \beta, t) = M(X, \beta, t) + E(X, t), \tag{4}$$

where H is the HDT fitting, M is the mathematical model fitting, E is the error fitting, X is the experimental data, β are the model parameters and t is the time.

3 Results

Figures 2, 3, and 4 display the results of peak temperatures at the exposure phase and minimum temperatures at the cooling phase, for Experiments 1, 2, and 3, respectively. The results obtained from the classical model are compared with those obtained from the HDT.

In Experiment 1, Training results are displayed. For peak temperatures, the classical model overestimates temperatures at the central points of the disk, where the highest temperatures are observed. Then it shows a sharp drop in temperature at intermediate radii values, which does not match the experimental data. Finally, it overestimates temperatures again at the external radii near the edge of the disk. However, the results from the HDT show a more accurate fit, particularly at the central points of the disk and intermediate radii. Regarding temperatures at the end of the cooling period, it is noticeable that the classical model again overestimates the results, while the HDT aligns much better with the experimental data.

In Experiment 2, Validation results are displayed. For peak temperatures, the classical model performs well at fitting temperatures at the center of the disk. However, it tends to underestimate temperatures for the rest of the points. It's worth noting that the HDT also fits the central points effectively but exhibits significantly higher precision for the remaining points. Regarding temperatures at the end of the cooling period, the classical model consistently underestimates them, whereas the HDT achieves temperatures similar to those observed in the experimental data.

In Experiment 3, Test results are displayed. Similar effects to the previous experiment are observed. However, in this instance, the accuracy of the HDT is slightly lower, especially for the temperatures at the end of the cooling period. This is to be expected, considering that the Test dataset is being utilized. Despite that, the HDT's performance remains notably better than that of the classical model.

Table 1 presents a comparison of result precision using the MAPE (Mean Absolute Percentage Error) metric. This comparison encompasses all times throughout each experiment, rather than focusing solely on two fixed times. The results confirm the observations made in Figures 2,3, and 4, as the MAPE of the HDT is substantially lower than that of the classical model.

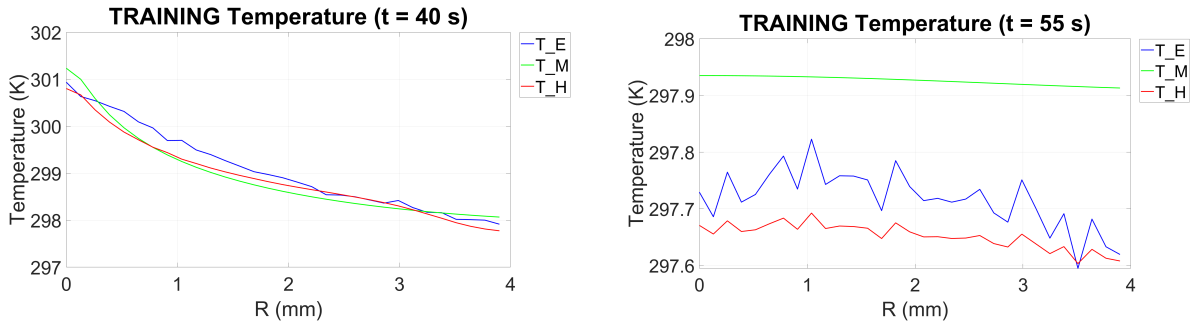

(a) (b)

Figure 2: Results of temperatures for Experiment 1, included in the Training dataset. (a) Peak temperature measured at time $t = 40$ s. (b) Temperature measured at the end of the cooling period at $t = 55$ s. T_{E} is the experimental temperature, T_{M} is the temperature output of the classical model, and T_{H} is the temperature output of the HDT.

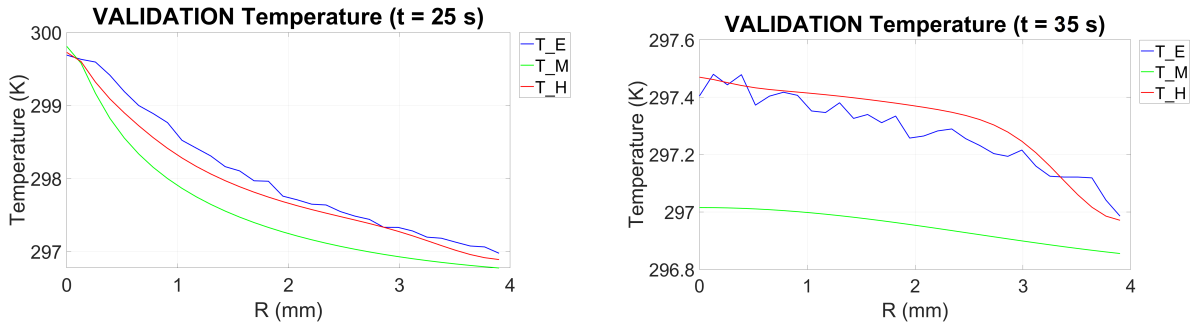

(a) (b)

Figure 3: Results of temperatures for Experiment 2, included in the Validation dataset. (a) Peak temperature of the second laser cycle (first validation cycle) at time $t = 25$ s. (b) Temperature measured at the end of the cooling period of the second cycle at $t = 35$ s. T_{E} is the experimental temperature, T_{M} is the temperature output of the classical model, and T_{H} is the temperature output of the HDT.

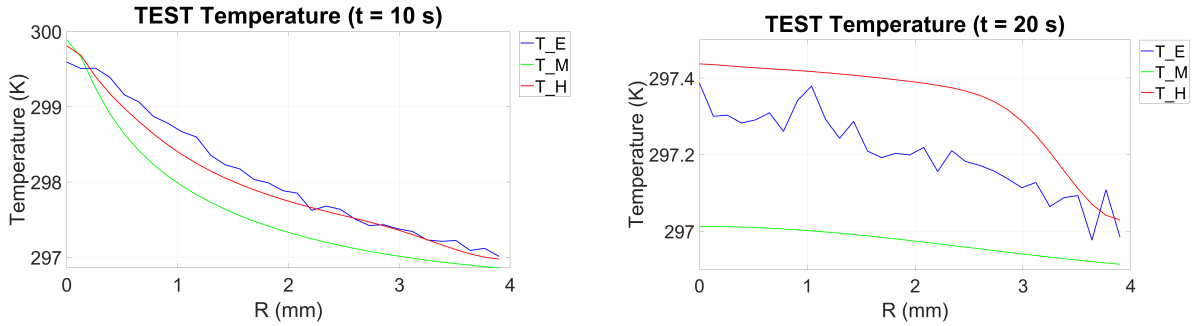

(a) (b)

Figure 4: Results of temperatures for Experiment 3, included in the Test dataset. (a) Peak temperature of the first laser cycle at time $t = 10$ s. (b) Temperature measured at the end of the cooling period of the first cycle at $t = 20$ s. T_{E} is the experimental temperature, T_{M} is the temperature output of the classical model, and T_{H} is the temperature output of the HDT.

Table 1: Comparison between the MAPE (Mean Absolute Percentage Error) of the Classic Model and the Hybrid Twins.

Dataset	classical Model	HDT	Improvement
Experiment 1 Training	0.0936	0.0317	66%
Experiment 2 Training	0.1095	0.0307	68%
Experiment 2 Validation	0.1278	0.0347	73%
Experiment 3 Test	0.0956	0.0408	57%

4 Conclusions

The implementation of the HDT methodology to a classical mathematical model has proven to be an effective strategy for enhancing the precision of the results without increasing the complexity of the model equations. Validation of the results has revealed that the adjustment made by HDT does not suffer from over-fitting, confirming its robustness and reliability in data prediction. Furthermore, the results in the Test dataset have shown that the adjustment made by HDT enables superior predictions compared to the classical model.

However, it should be noted that the HDT methodology has its limitations, such as the requirement for a well-defined model and a reasonably good initial fit of the data. Additionally, the adjustment process of HDT requires a higher computational and time cost as two adjustments are mandatory: one for the model and another for the error. Despite these limitations, HDT represents a promising tool for enhancing precision in the modeling of complex systems across various applications.

Acknowledgments

This work has been supported by the Spanish grant PID2020-115270GB-I00 granted by MCIN/A EI/10.12039/501100011033.

References

[1] D.L. Halaney, C.R. Jonak, J. Liu, N. Davoodzadeh, M.S. Cano-Velázquez, P. Ehtiyatkar, H. Park, D.K. Binder, and G. Aguilar, Chronic brain imaging across a transparent nanocrystalline yttria-stabilized-zirconia cranial implant, *Frontiers in Bioengineering and Biotechnology* 8 659 2020.

[2] I. Mellal, A. Oukaira, E. Kengene, and A. Lakhssassi, Thermal therapy modalities for cancer treatment: A review and future perspectives, *International Journal of Applied Science*, 4(2) 14 2017.

[3] Mildred S.Cano-Velázquez, Jose Bon, M.Llamazares, Santiago Camacho-López, Guillermo Aguilar, Juan Hernández-Cordero, MacarenaTrujillo, Experimental and computational model approach to assess the photothermal effects in transparent nanocrystalline yttria stabilized zirconia cranial implant, *Computer Methods and Programs in Biomedicine* 221 106896 2022.

[4] Francisco Chinesta, Elias Cueto, Emmanuelle Abisset-Chavanne, Jean Louis Duval, Fouad El Khaldi, Virtual, Digital and Hybrid Twins. A new paradigm in data-based engineering and engineered data, *Archives of Computational Methods in Engineering* 27(1) 2018.

[5] Marini, Federico and Walczak, Beata, Particle swarm optimization (PSO). A tutorial, *Chemometrics and Intelligent Laboratory Systems* 149 2015.

[6] Nuno Lourenco, Francisco B. Pereira, Ernesto Costa, Unveiling the properties of structured grammatical evolution, *Genetic Programming and Evolvable Machines* 17(3) 2016.

[7] Conor Ryan, Michael O'Neill, JJ Collins, Handbook of Grammatical Evolution, Springer 2018.